Available online at www.sciencedirect.com
ScienceDirect
journal homepage: www.elsevier.com/locate/burns

The effect of TGFβRI inhibition on fibroblast heterogeneity in hypertrophic scar 2D *in vitro* models

Rajiv S. Raktoe [a,*], *Marion H. Rietveld* [a], *Jacoba J. Out-Luiting* [a], *Marianna Kruithof-de Julio* [b,c], *Paul P.M. van Zuijlen* [d,e], *Remco van Doorn* [a], *Abdoelwaheb El Ghalbzouri* [a]

[a] *Department of Dermatology, Leiden University Medical Centre (LUMC), Leiden, the Netherlands*
[b] *Department of Urology, LUMC, Leiden, the Netherlands*
[c] *Department of Urology, University of Bern, Bern, Switzerland*
[d] *Amsterdam UMC Location VUmc, Department of Plastic, Reconstructive and Hand Surgery, Amsterdam Movement Sciences, Amsterdam, the Netherlands*
[e] *Burn Center and Department of Plastic and Reconstructive Surgery, Red Cross Hospital, Beverwijk, the Netherlands*

ARTICLE INFO

Article history:
Accepted 11 January 2021
Available online xxx

Keywords:
Hypertrophic scars
Fibroblast heterogeneity
Papillary fibroblast
Reticular fibroblast
Exon skipping
ALK5

ABSTRACT

In burn patients, wound healing is often accompanied by hypertrophic scarring (HTS), resulting in both functional and aesthetic problems. HTSs are characterized by abundant presence of myofibroblasts (MFs) residing in the dermis. HTS development and MF persistence is primarily regulated by TGF-β signalling. A promising method to target the transforming growth factor receptor I (TGFβRI; also known as activin-like kinase 5 (ALK5)) is by making use of exon skipping through antisense oligonucleotides. In HTS the distinguishing border between the papillary dermis and the reticular dermis is completely abrogated, thus exhibiting a one layered dermis containing a heterogenous fibroblast population, consisting of papillary fibroblasts (PFs), reticular fibroblasts (RFs) and MFs. It has been proposed that PFs, as opposed to RFs, exhibit anti-fibrotic properties. Currently, it is still unclear which fibroblast subtype is most affected by exon skipping treatment.

Therefore, the aim of this study was to investigate the effect of TGFβRI inhibition by exon skipping in PF, RF and HTS fibroblast monocultures.

Morphological analyses revealed the presence of a PF-like population after exon skipping in the different fibroblast cultures. This observation was further confirmed by the expression of genes specific for PFs, demonstrated by qPCR analyses. Further investigations on mRNA and protein level revealed that indeed MFs and to a lesser extent RFs are targeted by exon skipping. Furthermore, collagen gel contraction analysis showed that ALK5 exon skipping reduced TGF-β- induced contraction together with decreased alpha-smooth muscle actin expression levels.

Abbreviations: ACTA2, alpha-actin 2; ALK5, activin-like kinase 5; ALK5ViM, activin-like kinase 5 vivo-morpholino; AON, antisense oligonucleotide; αSMA, alpha-smooth muscle actin; CCRL1, c-c chemokine receptor type 11; CDH2, cadherin-2; CNN1, calponin-1; ECM, extracellular matrix; FPCL, fibroblast-populated collagen lattice; HTS, hypertrophic scar; MF, myofibroblast; NTN1, netrin-1; PF, papillary fibroblast; PDPN, podoplanin; RF, reticular fibroblast; SF, scar fibroblast; ScrViM, scrambled vivo-morpholino; TGM2, transglutaminase 2; TNC, tenascin-c; ViM, vivo-morpholino.

* *Corresponding author.*
E-mail address: rs.raktoe@gmail.com (R.S. Raktoe).

https://doi.org/10.1016/j.burns.2021.01.004

In conclusion, we show for the first time that exon skipping primarily targets pro-fibrotic fibroblasts. This could be a promising step towards reduced HTS development of burn tissue.

Introduction

The dermis of the skin is divided into two distinct layers; the superficial, papillary dermis and the deeper, reticular dermis with both layers differing in morphology and composition. The papillary dermis is mainly composed of loose matrix with high cell density. The fibroblasts present in this layer (PFs) exhibit a spindle- shape appearance when put in culture. The reticular dermis is composed of a dense matrix, consisting of mainly reticular fibroblasts (RFs) and low numbers of myofibroblasts (MFs). The latter types of fibroblasts have a flat square- shaped appearance when put in culture and express the biomarker alpha-smooth muscle actin (αSMA), of which MFs exhibit higher αSMA expression [1,2].

When trauma causes deep wounds, fibroblasts migrate towards the wound bed where they differentiate into MFs under the influence of transforming growth factor-β (TGF-β), an important regulator in skin homeostasis [3,4]. The main function of the MFs is to ensure wound healing by extracellular matrix (ECM) synthesis and contraction of the wound due to αSMA expression. Upon normal wound closure conditions, MFs enter apoptosis [3,5]. However, under pathological conditions, such as HTSs, the MFs remain active and produce excessive ECM components, in particular collagen type 1 and 3, leading to fibrotic tissue [6].

Furthermore, when comparing healthy skin to HTS tissue one can appreciate that the border between the papillary and reticular dermis, seen in healthy skin, is absent in HTS tissue due to replacement of both layers by scar tissue [7].

Extrapolating this knowledge to in vitro models, one encounters a heterogenic fibroblast population upon isolation of fibroblast from the dermis of HTS tissue, consisting of: PFs, RFs and MFs. Thus, when investigating the effects of anti-fibrotic therapies in scar fibroblast (SF) cultures, it is self-evident that one aims to target the MFs. However, questions remain about the differential susceptibility of PFs and RFs to the anti-fibrotic treatment due to the fact that these fibroblast subtypes also play a role in wound healing [8]. In addition, several studies have proposed that superficial fibroblasts, i.e., PFs, exhibit anti-fibrotic features [9–12]. Therefore, it would be of great interest to infer whether one is able to elevate PFs abundance and, thereby, inducing an anti-fibrotic effect in the SF culture.

Since the TGF-β signalling pathway plays a prominent role in HTS development and MFs activity [13,14]. In this this study, we interfere with the TGF-β pathway by inhibiting TGF-β type I receptor (TGFβRI), also known as activin-like kinase 5 (ALK5). Inhibition is established by specifically targeting exon 2, which encodes the ligand-binding domain of ALK5, using antisense oligonucleotides. This methodology results in a protein lacking the ligand-binding domain peptide sequence [15,16]. By targeting the TGF-β signalling pathway we aim to attenuate the activity of pro-fibrotic RFs and MFs, thereby proving anti-fibrotic PFs the upper hand.

By assessing the effects of TGF-βRI inhibition on the different fibroblast subpopulations in SFs cultures, one is able to provide more information on the functional differences between the subpopulation which could be a step forward in the development of a universal HTS treatment option that could allow reduced HTS development of burn tissue.

Materials and methods

Cell culture

Primary papillary fibroblasts (PFs) (N = 3) and reticular fibroblasts (RFs) (N = 3) were established from healthy abdominal or mammary tissue, obtained from cosmetic surgery. Based on the declaration of Helsinki principles patient consent was not required since the excised scar tissue was considered as waste material. Experiments were conducted in accordance with article 7:467 of the Dutch Law on Medical Treatment Agreement and the Code for proper Use of Human Tissue of the Dutch Federation of Biomedical Scientific Societies (https://www.federa.org/codes-conduct). As of this national legislation, coded surplus tissue and HTS tissue can be used for scientific research purposes when no written objection is made by the informed donor. Therefore, additional approval of an ethics committee regarding scientific use of excised HS tissue was not required. Thus, no specific approval by institutional ethics committee was requested.

Isolation of the PFs and RFs was performed as described earlier [17]. In short, the papillary and reticular layer were separated using a dermatome at two different depths. A layer of 300 μm thickness, containing the epidermis and papillary layer of which the epidermis was discarded. The second layer was dermatomed at a depth of 700 μm containing the reticular layer. Next, the dermal layers were incubated in Collagenase (Invitrogen, Breda, the Netherlands) and dispase (Roche Diagnostics, Almere, the Netherlands), mixed in a 3:1 ratio for 2 h at 37 °C. Next, PFs and RFs were isolated.

HTS tissue from three donors was used to isolate the heterogenic fibroblast population consisting of PFs, RFs and myofibroblasts (MFs) and will be referred as scar fibroblasts (SFs). As for the SFs, HTS tissue was cut in pieces of 0.5 cm × 0.5 cm and incubated overnight in dispase II at 4 °C and subsequently incubated for 30 min at 37 °C for separation of the epidermis from the dermis. Next, the dermal compartment was incubated with Collagenase (Invitrogen, Breda, the Netherlands) and dispase (Roche Diagnostics, Almere, the Netherlands), mixed in a 3:1 ratio for 2 h at 37 °C and the SFs were isolated. The PFs, RFs and SFs were cultured in Dulbecco's Modified Eagle's Medium (DMEM) (Gibco/ Invitrogen, Breda,

Please cite this article in press as: R.S. Raktoe, et al., The effect of TGFβRI inhibition on fibroblast heterogeneity in hypertrophic scar 2D *in vitro* models, Burns (2021), https://doi.org/10.1016/j.burns.2021.01.004

the Netherlands) supplemented with 5% fetal bovine serum (FBS; HyClone, Thermo Scientific, Etten-Leur, the Netherlands) and 1% penicillin–streptomycin (Thermo Fisher Scientific, Massachusetts, United States). The fibroblasts were kept at 37 °C and 5% CO2 and used for following experiments between the 3rd and 5th passage.

Next, fibroblasts were plated on 6 cm dished in a density of 5×10^4 cells per dish and cultured for 24 h. The fibroblasts were then deprived from serum overnight to be sequentially treated with recombinant human TGF-β1 (5 ng/ml; Cell Signalling Technology) and incubated for 24 h. Next, the fibroblasts were treated with antisense oligonucleotides, consisting of a scrambled sequence (ScrViM; 2 μM) or exon 2 specific sequence (ALK5ViM; 2 μM), or pharmacological ALK5 inhibitor SB431542 (10 μM). The sequences (5′-3′) of the ViM's are the following: ALK5ViM: GCAGTGGTCCTGATTGCAGCAATAT, ScrViM: CCTCTTACCTCAGTTAC AATTTATA. After 24 h of incubation culture medium was refreshed and incubated for an additional three days. Samples were harvested for sequential analysis.

RNA and protein isolation

The fibroblast monolayer cultures were lysed for RNA and protein extraction performed with the Favorgen® (Biotech corp., Ping-Tung, Taiwan) extraction kit and Tissue Protein Extraction Reagent (T-PER, Thermo Scientific, Massachusetts, United States), respectively. Isolations were performed according to manufacturer's protocol.

Quantitative RT-PCR

Total RNA was used for cDNA synthesis, using the iScript™ cDNA Synthesis Kit (Bio-Rad Laboratories Inc., Hercules, California, United States). For qPCR analysis, the cDNA was amplified in a CFX Real Time Detection system (Bio-Rad Laboratories Inc., Hercules, California, United States) using SYBR Green Supermix reagent (Bio-Rad Laboratories Inc., Hercules, California, United States). Expression levels of the following genes were determined: CCRL1, (C-C chemokine receptor type 11), NTN1 (Netrin-1), PDPN (Podoplanin), TNC (Tenascin-C), CNN1 (Calponin 1), CDH2 (Cadherin-2), Transglutaminase 2 (TGM2) and ACTA2 (actin-alpha 2). The expression levels were normalized to reference genes EI24 (Etoposide Induced 2.4), SDHA (Succinate Dehydrogenase Complex Flavoprotein Subunit A), GOLGA1 (golgin A1), SND1 (Staphylococcal Nuclease And Tudor Domain Containing 1) and the relative normalized expression levels were calculated using Bio-rad CFX Manager™ Version 3.1 (Bio-Rad Laboratories Inc., Hercules, California, United States).

Western Blot

Loading buffer was added 10 μg of each sample and heated to 100 °C for five minutes. After a brief centrifugation, the samples were loaded on MINI-PROTEAN precast gels (Bio-Rad Laboratories B.V., Veenendaal, Netherlands) for electrophoresis. Next, protein was transferred onto a Polyvinylidene difluoride (PVDF) membrane (Bio-Rad Laboratories B.V., Veenendaal, Netherlands) for seven minutes at room temperature using the Trans-Blot® Turbo™ Transfer System (Bio-Rad Laboratories B.V., Veenendaal, Netherlands). Subsequently, membranes were incubated with the following primary antibodies overnight at four degrees: Tenascin-C (TNC) (1:750; Novus Biologicals, Centennial, Colorado, United States), Transglutaminase 2 (TGM2) (1:750; Abcam, Cambridge, United Kingdom) and alpha- smooth muscle actin (αSMA) (1:500; Progen, Heidelberg, Germany). For western blot analysis to assess basal biomarker levels prior to treatment, the following antibodies were used: PDPN (1:500; Santa Cruz Biotechnology, Texas, United States), CDH2 (1:1000; Thermo Scientific, Massachusetts, United States) and αSMA (1:500; Progen, Heidelberg, Germany).

Glyceraldehyde 3-phosphate dehydrogenase (GAPDH) (1:1500, Cell Signaling, Massachusetts, United States) was used as a loading control. The membranes were then incubated with a secondary antibody (Pierce, anti-mouse IgG and anti-rabbit IgG HRP-conjugated, 1:2500 diluted in blocking buffer) for 60 min. at RT and prepared for visualization using enhanced chemiluminescence (ECL) substrate solution (Pierce, SuperSignal West Femto Maximum Sensitivity Substrate) in a dark environment. Visualization was performed with the ChemiDoc™ MP System (Bio-Rad Laboratories B.V., Veenendaal, Netherlands).

Contraction of fibroblast populated collagen lattices

Rat collagen was extracted from tail tendons of which the procedure is described previously [18]. Fibroblast populated collagen lattices (FPCL) were established by embedding PFs (N = 3), RFs (N = 3) and SFs (N = 3) into a rat collagen matrix (4 mg/ ml) at a seeding density of 4×10^4 cells/ ml. The FPCLs were cultured for 24 h at 37 °C and 5% CO_2.

Next, the FPCLs were serum deprived O/N (DMEM, containing 0.5% FBS; 1% P/S). Serum deprivation was followed by TGF-β1 (5 ng/ ml) treatment for 6 h and lattices were sequentially treated with ScrViM (4 μM), ALK5ViM (4 μM) or SB431542 (10 μM) for 24 h. After 24 h of treatment, the collagen lattices were refreshed with normal culture medium (DMEM, containing 5% FBS; 1% P/S) and cultured for an additional 72 h and harvested. Macroscopic imaging was performed using a 12-megapixel camera mounted on a Samsung Galaxy S7 mobile phone (Samsung Electronics Co., Ltd., Daegu, South Korea). Images were analyzed using ImageJ and average ration was calculated, in order to quantify the amount of contraction. Ratio was calculated by dividing the area of the collagen lattice (in pixel) by the area of the well (in pixel).

αSMA immunofluorescence staining of FPCLs

Formalin-fixed FPCL cross sections of 5 μm were stained for αSMA by immunofluorescence.

The FPCL sections were de-paraffinized, rehydrated and incubated with αSMA (alpha-smooth muscle actin; 1:500; Progen, Heidelberg, Germany) primary antibody O/N at 4ºC. Primary staining was then followed by secondary antibody incubation (Cy™3 AffiniPure Goat Anti-Mouse; 1:250; Jackson Immunoresearch Laboratories Inc., Camebridgeshire, United Kingdom) for 1 h at RT. After antibody incubation, the cells

Please cite this article in press as: R.S. Raktoe, et al., The effect of TGFβRI inhibition on fibroblast heterogeneity in hypertrophic scar 2D *in vitro* models, Burns (2021), https://doi.org/10.1016/j.burns.2021.01.004

were washed with PBS and counterstained the nuclei using 4',6-diamidino-2-phenylindole (DAPI; 1:4000; Carlsbad, California, United States) and mounted for visualization with mounting medium that preserves fluorescence (VECTASHIELD, VECTOR Laboratories, Burlingame, California). Quantification of αSMA expression was performed with ImageJ software. The positive area fraction was calculated by setting an upper and lower threshold, in order to count the pixels exhibiting a positive fluorescent signal.

Statistics

The obtained data was transferred to GraphPad Prism version 8.00 for Windows (GraphPad Software, California, United States). mRNA expression data was analysed using a multiple t-test – one per row. Statistical analysis on collagen gel contraction and αSMA immunofluorescence signal were conducted using a two-way ANOVA test. To adjust for multiple comparisons, we have used the Holm-Šídák multiple comparisons test. The differences were noted as follows: $P \leq 0.05$, *; $P \leq 0.01$, **; $P \leq 0.001$, ***.

Results

Papillary fibroblasts alter in morphology and biomarker gene expression after exon skipping

In order to investigate if exon skipping could induce a shift in PF and RF biomarkers, we conducted gene expression analysis on a panel of biomarkers that were reported by Janson et al. to be specific for both fibroblast subtypes [1]. For PFs we used CCRL1, NTN1, PDPN and TNC as biomarkers, while for validation of RFs we have used CNN1, CDH2 and TGM2 as biomarkers. To distinguish MFs from RFs and PFs, we used solely ACTA2 as a biomarker.

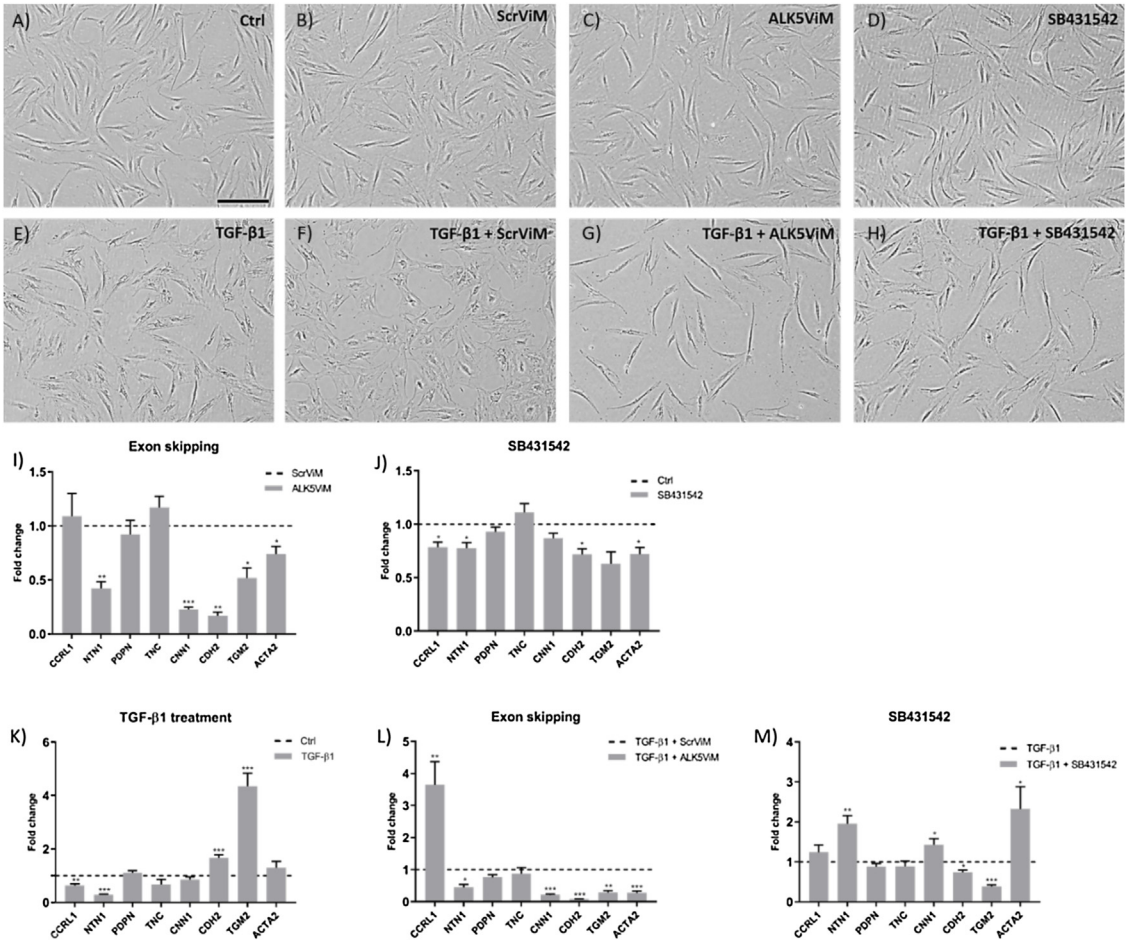

Fig. 1 – Brightfield microscopy images and gene expression analysis on PFs. **(A–H) Images of PFs at basal level (A-D) or stimulated with TGF-β (E-H). Scale bar: 100 μm. (I and J) Relative normalized fold change expression of PF (CCRL1, NTN1, PDPN and TNC), RF (CNN1, CDH2 and TGM2) and MF (ACTA2) markers after exon skipping and pharmacological inhibition at basal level. (K) Effect of TGF-β1 activation displaying normalized relative fold change expression of PF, RF and MF markers. (E and F) Effect of exon skipping and pharmacological inhibition after TGF-β1 stimulation on relative normalized fold change expression levels of fibroblast markers. The graph represents the relative normalized mRNA expression values of the treated samples over their putative control samples (set at one; dashed line). N = 3; error bars represent standard error of the mean (SEM); *$P \leq 0.05$; **$P \leq 0.01$; ***$P \leq 0.001$; multiple t-test.**

First, we assessed changes in PF morphology after 96 h. In non- TGF-β-treated PFs (Fig. 1A–D) exon skipping (Fig. 1C) did not affect fibroblast morphology, compared to untreated (Fig. 1A), ScrViM- treated (Fig. 1B) samples. TGF-β1- stimulated PFs (Fig. 1E–H) showed a polygonal shape (star-like shape) (Fig. 1E), resembling RFs. Sequential exon skipping (Fig. 2G) showed that the shape of the fibroblasts obtained a spindle-shape morphology, hence resembling PFs. A similar observation was found after SB431542 treatment.

To confirm our observations, we validated fold change mRNA expression levels of the biomarkers (Fig. 1I–M). First, we investigated the effects of ALK5 exon skipping without TGF-β stimulation (Fig. 1I). Pharmacological ALK5 inhibitor SB431542 was used as a positive control (Fig. 1J). Here, we found that both RFs markers CNN1, CDH2, TGM2, PF marker NTN1 and MF marker ACTA2 were significantly downregulated (CNN1; $P \leq 0.001$, CDH2; $P \leq 0.01$, TGM2; $P \leq 0.05$, NTN1; $P \leq 0.05$ and ACTA2 $P \leq 0.05$) after exon skipping. SB431542 showed downregulation of CCRL1 ($P \leq 0.05$), NTN1 ($P \leq 0.05$), CDH2 ($P \leq 0.05$) and ACTA2 ($P \leq 0.05$) (Fig. 1J). Next, we assessed the effect of TGF-β1 treatment (Fig. 2K). We found an elevation of RF markers CDH2 ($P \leq 0.001$) and TGM2 ($P \leq 0.001$) and a significant downregulation of PF biomarkers CCRL1 ($P \leq 0.001$) and NTN1 ($P \leq 0.001$). No significant elevation of MF marker ACTA2 was found. Sequential exon skipping (Fig. 1L) showed a significant upregulation of PF marker CCRL1 ($P \leq 0.05$) and downregulation of NTN1 ($P \leq 0.05$). RF (CNN1; $P \leq 0.001$, CDH2; $P \leq 0.001$ and TGM2; $P \leq 0.01$) and MF (ACTA2; $P \leq 0.001$) markers were all significantly downregulated after exon skipping. SB431542 showed a significant upregulation of PF marker NTN1 ($P \leq 0.01$) and RF marker TGM2 ($P \leq 0.001$). Both RF and MF markers CNN1 ($P \leq 0.05$) and ACTA2 ($P \leq 0.05$) were upregulated in the SB431542 treated group (Fig. 1M).

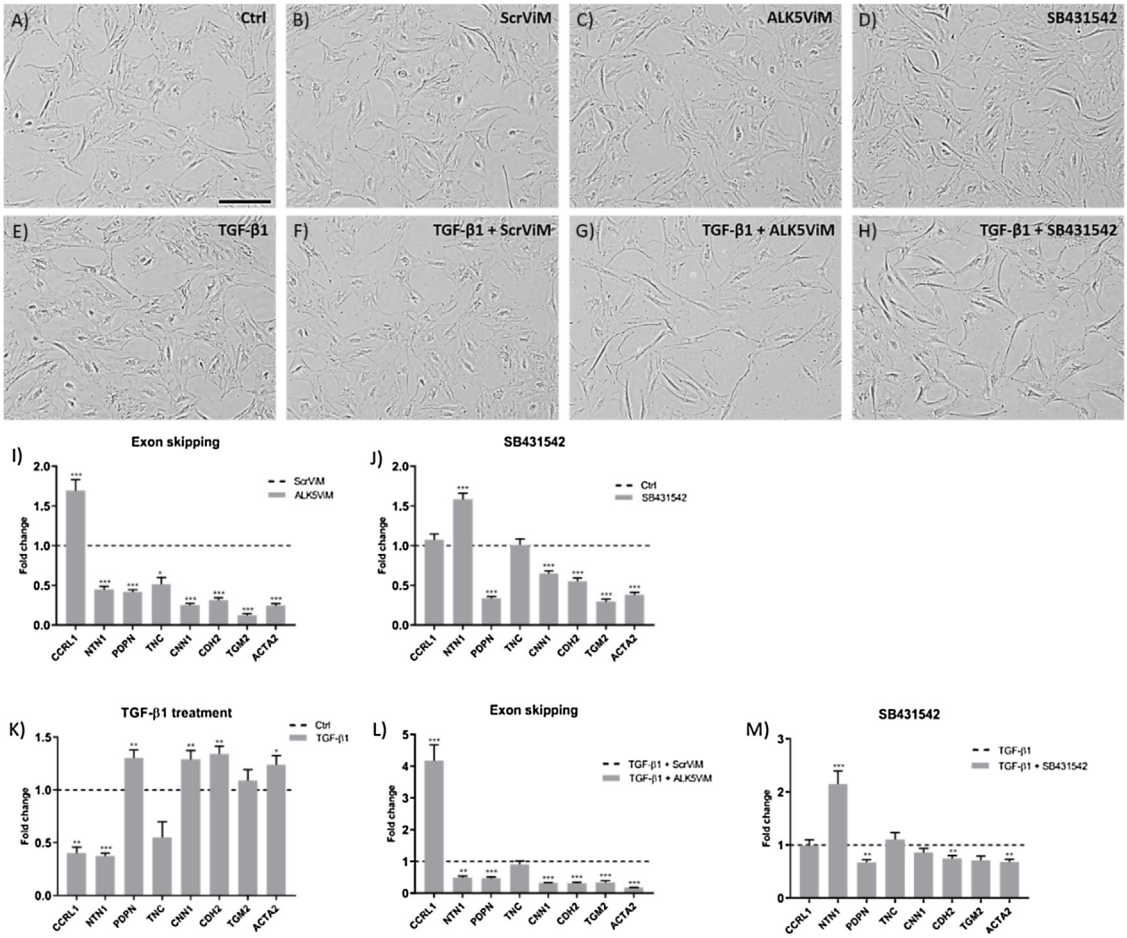

Fig. 2 – Brightfield microscopy images and gene expression analysis on RFs. **(A–D) Morphology of non-TGF-β- treated RFs. (E–H) Images of TGF-β stimulated RFs. Scale bar: 100 μm. (I and J) Relative normalized fold change expression of PF (CCRL1, NTN1, PDPN and TNC), RF (CNN1, CDH2 and TGM2) and MF (ACTA2) markers after exon skipping and pharmacological inhibition at basal level. (K) Effect of TGF-β1 activation displaying normalized relative fold change expression of PF, RF and MF markers. (E and F) Effect of exon skipping and pharmacological inhibition after TGF-β1 stimulation on relative normalized fold change expression levels of fibroblast markers. The graph represents the relative normalized mRNA expression values of the treated samples over their putative control samples (set at one; dashed line). N = 3; error bars represent standard error of the mean (SEM); *P ≤ 0.05; **P ≤ 0.01; ***P ≤ 0.001; multiple t-test.**

Please cite this article in press as: R.S. Raktoe, et al., The effect of TGFβRI inhibition on fibroblast heterogeneity in hypertrophic scar 2D *in vitro* models, Burns (2021), https://doi.org/10.1016/j.burns.2021.01.004

Exon skipping affects reticular fibroblast morphology and gene expression

Next, we assessed the effect of exon skipping on RFs. Brightfield microscopy images revealed that there were no changes in morphology at basal level (Fig. 2A–D). However, in the TGF-β-stimulated samples (Figs. 2E–H) we observed that after exon skipping (Fig. 2G) the fibroblasts showed a more spindle-shape like appearance, compared to TGF-β stimulation (Fig. 2E) and sequential ScrViM treatment (Fig. 2F). Sequential SB431542 treatment after TGF-β stimulation showed little presence of spindle-shaped fibroblasts (Fig. 2H).

mRNA expression analysis of the different fibroblast markers of the samples at basal level (Fig. 2I) showed that after exon skipping (Fig. 2C) RF markers (CNN1; $P \leq 0.001$, CDH2; $P \leq 0.001$ and TGM2; $P \leq 0.001$) and the MF marker ACTA2 ($P \leq 0.001$) were significantly downregulated. In addition, we found that three out of four PF markers were significantly downregulated (NTN1; $P \leq 0.001$, PDPN; $P \leq 0.001$ and TNC; $P \leq 0.05$), whereas CCRL1 was upregulated (CCRL1; $P \leq 0.001$). SB431542 treatment (Fig. 2J) showed a similar effect on RF and MF markers as was found with exon skipping. As for the PF marker PDPN, we found a significant downregulation when treated with SB431542 ($P < 0.001$) and upregulation of NTN1 ($P < 0.001$).

Upon TGF-β activation (Fig. 2K) PF markers CCRL1 ($P \leq 0.01$) and NTN1 ($P \leq 0.001$) were substantially downregulated, whereas PDPN was upregulated ($P \leq 0{,}01$). Further, both RF markers (CNN1; $P \leq 0.05$ and CDH2; $P \leq 0.01$) and MF marker (ACTA2; $P \leq 0.05$) were significantly upregulated. When TGF-β-stimulated RFs were sequentially treated with ALK5ViM (Fig. 2L), we found that all RF and MF markers were substantially downregulated (CNN1; $P \leq 0.001$, CDH2; $P \leq 0.001$, TGM2; $P \leq 0.001$ and ACTA2, $P \leq 0.001$). Expression levels for PF markers showed a similar effect as found in non TGF-β- stimulated RFs (Fig. 2I). When TGF-β activation was followed by SB431542 treatment (Fig. 2M), the effect on PF markers was similar as determined for SB431542 at basal level. Further, SB431542 treatment induced significant downregulation of RF marker CDH2 ($P \leq 0.01$) and MF markers ACTA2 ($P \leq 0.01$).

Exon skipping induces a shift in fibroblast markers in scar fibroblasts

Next, fibroblasts derived from HTS tissue were examined. As shown in Fig. 3A, the dermis of normal human skin displays a clear border between the papillary (I) and reticular dermis (II). This makes it relatively easy to isolate fibroblasts from the respective dermal layers. However, in the dermis of HTS tissue this border is absent (Fig. 3B; III), which makes it impossible to macroscopically distinguish between PFs, RFs and MFs. Therefore, we isolated the complete HTS fibroblast population referred to SFs.

Morphology of the SFs at basal level showed abundance of spindle-shaped fibroblasts and to lower extent presence of polygonal shaped fibroblasts (Fig. 4A–D). Treatment with ALK5ViM or SB431542 did not affect the morphology of the fibroblasts. Upon TGF-β activation (Fig. 4E), we found that fibroblast morphology obtained an overall polygonal appearance and sequential treatment with the control oligonucleotide ScrViM did not affect fibroblast morphology (Fig. 4F). However, when TGF-β- stimulated SFs were treated with ALK5ViM we observed a shift in morphology towards a spindle-shape like appearance (Fig. 4G). A similar effect was found after SB431542 treatment (Fig. 4H).

Gene expression analysis at basal level showed that exon skipping only showed a downregulation in RF marker CNN1 ($P \leq 0.001$) and MF marker ACTA2 ($P \leq 0.001$) (Fig. 4I). Pharmacological inhibitor SB431542 showed substantial upregulation of PF markers CCRL1 ($P \leq 0.05$), NTN1 ($P \leq 0.05$) and PDPN ($P \leq 0{,}01$) (Fig. 4J). TCN was downregulated in the SB431542 treated group ($P \leq 0.01$). Further, pharmacological ALK5 inhibition showed downregulation of TGM2 ($P \leq 0.01$) and ACTA2 ($P \leq 0.01$).

Next, SFs were activated with TGF-β1 (Fig. 4K) and we found a significant downregulation of PF markers CCRL1 ($P \leq 0.001$), NTN1 ($P \leq 0.01$) and elevated TNC expression levels ($P \leq 0.05$). All RF markers (CNN1; $P \leq 0.001$, CDH2; $P \leq 0.001$ and TGM2; $P \leq 0.001$) together with MF marker (ACTA2; $P \leq 0.001$) were significantly upregulated. Sequential exon skipping (Fig. 4L) showed a substantial downregulation of RF markers CNN1 ($P \leq 0.001$), CDH2 ($P \leq 0.001$) and MF marker ACTA2 ($P \leq 0.001$). Further, ALK5ViM induced significant elevation of PF markers

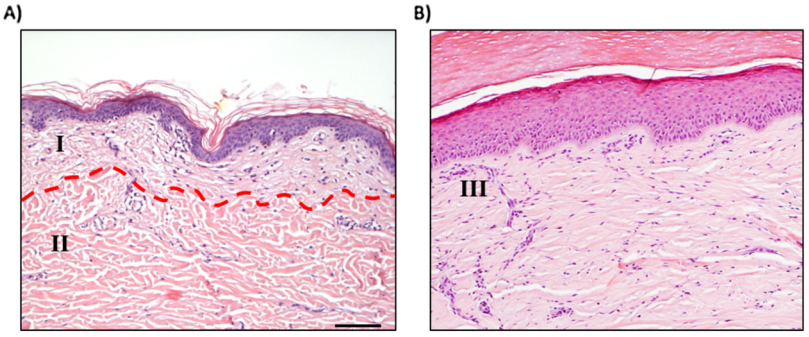

Fig. 3 – Histological characteristics of the dermis of normal skin and HTS tissue. **(A) Hematoxylin and Eosin staining of normal skin. The red line displays the border between the two layers of the dermis: (I) Papillary dermis and (II) Reticular dermis. (B) Dermis of HTS tissue where the border between the papillary and reticular layer is abrogated due to replacement of scar tissue B (III). Scale bar: 100 μm (For interpretation of the references to colour in this figure legend, the reader is referred to the web version of this article).**

Please cite this article in press as: R.S. Raktoe, et al., The effect of TGFβRI inhibition on fibroblast heterogeneity in hypertrophic scar 2D *in vitro* models, Burns (2021), https://doi.org/10.1016/j.burns.2021.01.004

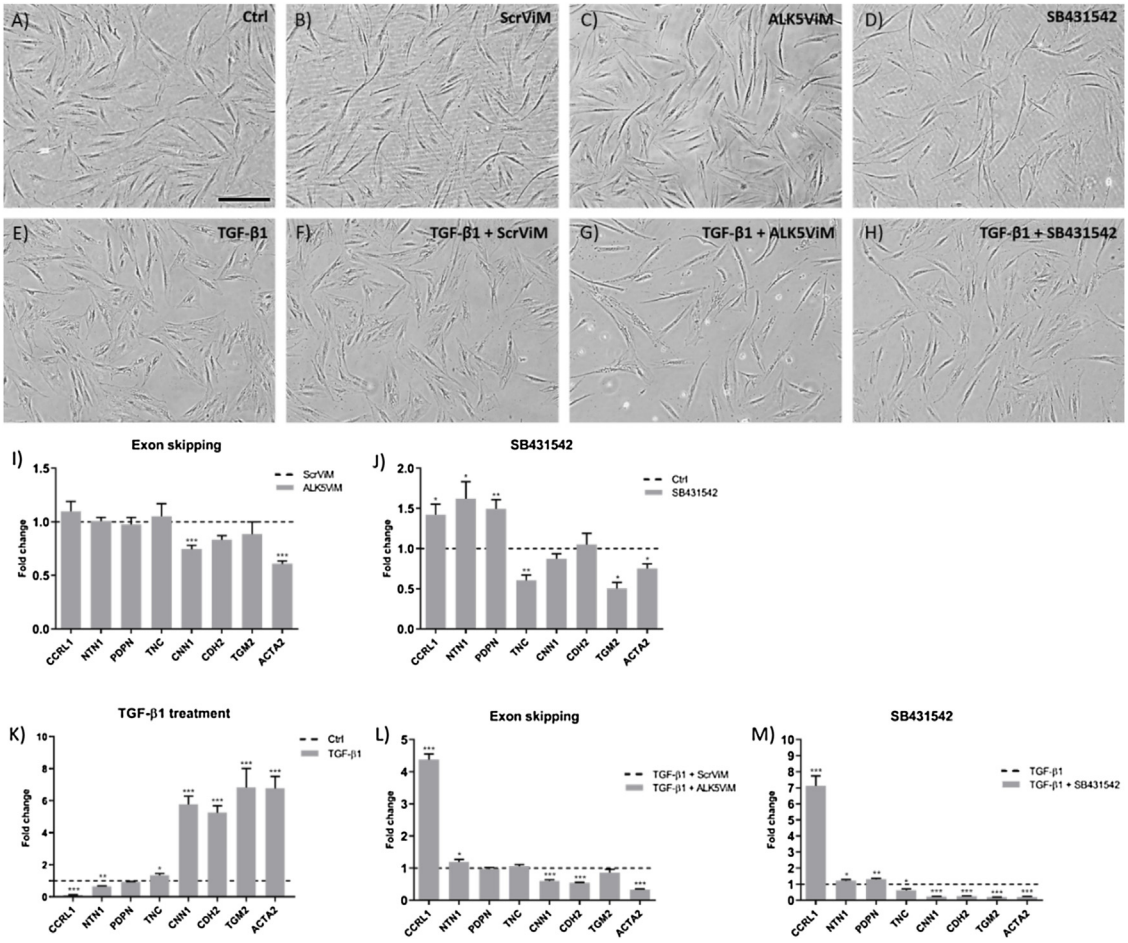

Fig. 4 – Morphology and gene expression analysis on SFs. **(A-D) Morphology of SFs at basal level. (E-H) TGF-β activated SFs. Scale bar: 100 μm. (I and J) Relative normalized fold change expression of PF (CCRL1, NTN1, PDPN and TNC), RF (CNN1, CDH2 and TGM2) and MF (ACTA2) markers after exon skipping and pharmacological inhibition at basal level. (K) Effect of TGF-β1 activation displaying normalized relative fold change expression of PF, RF and MF markers. (E and F) Effect of exon skipping and pharmacological inhibition after TGF-β1 stimulation on relative normalized fold change expression levels of fibroblast markers. The graph represents the relative normalized mRNA expression values of the treated samples over their putative control samples (set at one; dashed line). N = 3; error bars represent standard error of the mean (SEM); *P ≤ 0.05; **P ≤ 0.01; ***P ≤ 0.001; multiple t-test.**

CCRL1 ($P \leq 0.001$) and NTN1 ($P \leq 0.05$). PDPN and TNC expression levels were not affected. Further, SB431542 showed a significant downregulation of all RF markers ($P \leq 0.001$) and ACTA2 ($P \leq 0.001$) expression levels (Fig. 4M). Furthermore, SB431542 showed a significant upregulation of CCRL1 ($P \leq 0.001$), NTN1 ($P \leq 0.05$), PDPN ($P \leq 0.01$) and TNC ($P \leq 0.05$).

TGF-β1- activated papillary fibroblasts, reticular fibroblasts and scar fibroblasts show reduced tenascin-C (TNC) expression after exon skipping

After confirmation at gene expression level, we continued with protein expression of fibroblast biomarkers. Therefore, we selected the PF marker tenascin-C (TNC) and RF marker transglutaminase 2 (TGM2), since these proteins have been reported to be highly expressed in PFs and RFs, respectively. αSMA was used as a biomarker for MFs [19].

Fig. 5 shows western blots of the different fibroblast markers TNC, TGM2, αSMA and reference protein GAPDH at basal level and after TGF-β1 activation in the different fibroblast cultures. Because of high donor variability, no statistical significant differences were found between conditions. However, for some conditions a clear trend was observed.

In PFs (Fig. 5A) we observed a reduction in TNC protein expression after exon skipping. This effect was most pronounced in the TGF-β- stimulated group. Although, sequential SB431542 treatment showed a reduction in TNC expression to a lesser extent. TGM2 showed overall weak expression at basal level. In the TGF-β-stimulated group, we observed a slight reduction in TGM2 expression after treatment with ScrViM and ALK5ViM. After SB431542 treatment, two out of three donors exhibited substantial downregulation of TGM2. MF marker αSMA was evenly downregulated by ScrViM and

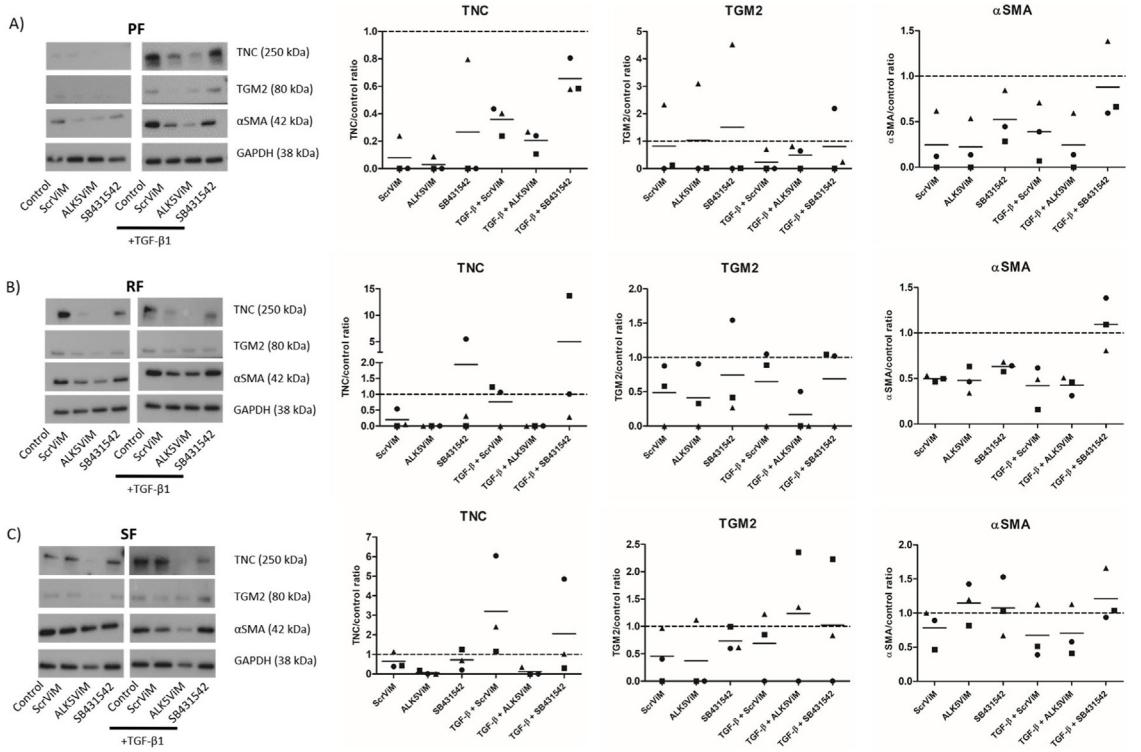

Fig. 5 – Immunoblotting of fibroblast marker expression in the different fibroblast cultures. **Representative western blots and quantification for (A) PFs (N = 3), (B) RFs (N = 3) and (C) SFs (N = 3). For all fibroblast cultures the expression of TNC (PF marker), TGM2 (RF marker) and αSMA (MF marker) was assessed. GAPDH was used as a loading control. Relative intensity of TNC, TGM2 and αSMA was calculated by dividing the band intensity of the protein of interest by the corresponding GAPDH band intensity. Normalization was performed by dividing the relative band intensity of the treatment by their respective control samples (Ctrl or TGF-β, set at one; dashed line). Each symbol shape represents a different donor.**

ALK5ViM at basal level and to lesser extent by SB431542 treatment. In the TGF-β-activated group exon skipping induced a substantial reduction of αSMA in two out of three donors.

In RFs (Fig. 5B) we observed a considerable reduction in TNC expression after exon skipping in the TGF-β-stimulated group. TGM2 showed overall weak protein expression on the immunoblots, however after quantification we observed a similar effect of ALK5 exon skipping in the TGF-β-activated group as was found observed for TNC. No large changes were observed after SB431542 treatment. Further, no changes were found in αSMA expression after ALK5 inhibition in the non TGF-β-treated and TGF-β-treated group.

Regarding the SF cultures (Fig. 5C), a similar effect was observed on TNC expression by ALK5 exon skipping as was found in PF and RF cultures. Further, as reported earlier for TGM2 expression, overall weak expression was observed. At basal level, a similar trend was observed in TGM2 expression as was observed in RFs. In the TGF-β- stimulated group two out of three donors were upregulated compared to the control sample after ALK5 exon skipping. As for αSMA, ALK5 exon skipping showed a slight increase in protein expression at basal level. TGF-β activation followed by ScrViM, ALK5ViM or SB431542 treatment showed a similar reduction in αSMA expression as was observed in RFs.

Differential effect on collagen contraction by fibroblast subtypes

Next, we investigated the extent to which the different fibroblast subtypes affect contraction and if we could inhibit contraction using exon skipping. Therefore, we established FPCLs in which we embedded PFs, RFs or SFs and assessed the extent of contraction (Fig. 6A–D). In addition, we assessed whether changes in contraction correlated with αSMA expression (Fig. 6E–G).

PF-containing collagen lattices (Fig. 6A) showed 25% contraction at basal level compared to the RF- (Fig. 6B) and SF- based collagen lattices (Fig. 6C). TGF-β1 stimulation showed a slight increase in contraction of the PF- containing collagen gel, however, not significant (Fig. 6A; TGF-β). Following TGF-β stimulation with sequential ScrViM treatment, did not show any substantial changes in contraction (Fig. 6A; TGF-β + ScrViM). Sequential exon skipping treatment (Fig. 6A; TGF-β + ALK5ViM) showed a significant reduction in contraction compared to the control condition ($P \leq 0.001$) (Fig. 6D). Although not significant, SB431542 treatment substantially reduced contractility compared to control conditions (Fig. 6A; SB431542 and TGF-β + SB431542). αSMA expression showed no dramatic changes between the different conditions (Fig. 6E).

Please cite this article in press as: R.S. Raktoe, et al., The effect of TGFβRI inhibition on fibroblast heterogeneity in hypertrophic scar 2D *in vitro* models, Burns (2021), https://doi.org/10.1016/j.burns.2021.01.004

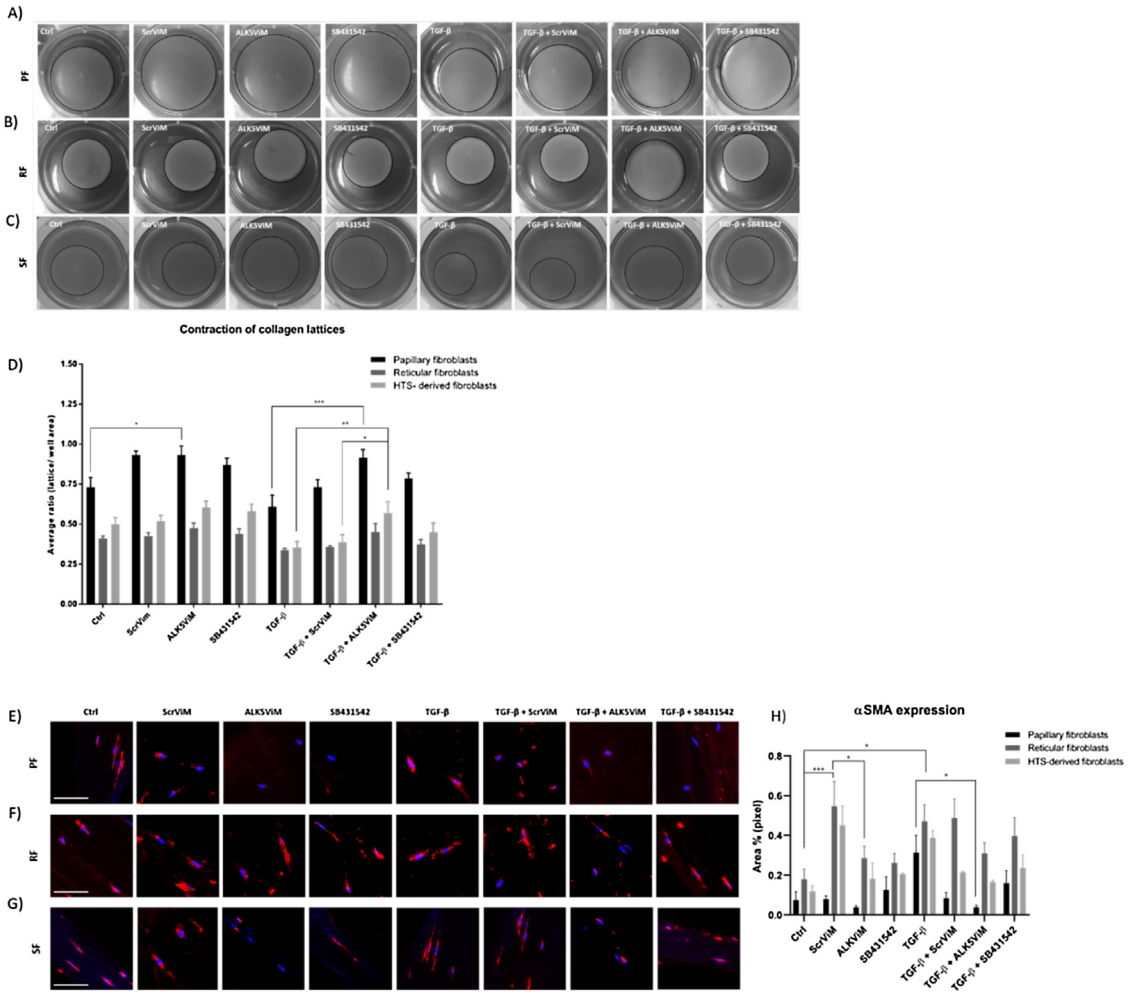

Fig. 6 – Contraction assay of FPCLs established with PFs, RFs or SFs. **(A–C) Images of the different FPCLs after 96 h. The type of treatment is indicated in the upper left corner of each image (D) Analysis of contraction of the different collagen lattices after 96 h. Quantification was performed using ImageJ. The amount of contraction was calculated by dividing the area of the lattice (in pixels) by the area of the well (pixels). The bar graphs represent the average ration of the different fibroblast populations: PF (black), RF (dark grey) and SF (grey). (E–H) Immunofluorescence staining for αSMA on the different FPCLs and quantification of the αSMA positive area. Total magnification of the images: 200 ×. N = 3 per fibroblast population; error bars represent standard error of the mean (SEM); *P ≤ 0.05; **P ≤ 0.01; ***P ≤ 0.001; two-way ANOVA.**

The collagen lattices embedded with RFs (Fig. 6B) showed high contraction at basal level, compared to PF collagen lattices (Fig. 6D). Exon skipping did not show any reduction at basal level (Fig. 6B; ALK5ViM). In addition, TGF-β1 stimulation (Fig. 6B; TGF-β) did not show major effects on contractility of the collagen lattices. Exon skipping showed a slight reduction in contraction of the RF collagen lattices (Fig. 6B; TGF-β + ALK5ViM), whereas the pharmacological inhibitor was not able to counteract the effect of TGF-β1 (Fig. 6B; TGF-β + SB431542). αSMA immunofluorescence staining showed that RF containing lattices (Fig. 6F) exhibited higher expression levels compared to PF embedded lattices (Fig. 6E). ALK5 inhibition did not affect αSMA expression in RF containing FPCLs.

SF- containing collagen lattices (Fig. 6C) showed overall significant contraction, compared to PF collagen gels ($P \leq 0.001$) (Fig. 6D). Furthermore, exon skipping and pharmacological ALK5 inhibition showed a slight reduction in contraction at basal level (Fig. 6C; ALK5ViM and SB431542; Fig. 6D) compared to control samples. Furthermore, TGF-β1 stimulation showed high contractility (Fig. 6C; TGF-β, TGF-β + ScrViM and Fig. 6D). The effect of TGF-β1 was counteracted with ALK5 exon skipping, compared to TGF-β1 treated samples ($P \leq 0.01$) and TGF-β1 + ScrViM samples ($P \leq 0.05$) (Fig. 6C and D). SB431542 showed a slight reduction in contraction compared to TGF-β1 treated samples, however, this effect was not as pronounced as with exon skipping. Furthermore, αSMA expression in the FPCLs followed the changes in contraction that were calculated in Fig. 6D (Fig. 6E–G). Quantification of IF images (Fig. 6H) revealed that PF-containing FPLCs possessed lower αSMA compared to whereas RF- and SF-containing FPLCs.

Please cite this article in press as: R.S. Raktoe, et al., The effect of TGFβRI inhibition on fibroblast heterogeneity in hypertrophic scar 2D *in vitro* models, Burns (2021), https://doi.org/10.1016/j.burns.2021.01.004

Discussion

In this study, we aimed to unravel which dermal fibroblasts subtype is affected by exon skipping. Numerous studies have investigated the differential expression profiles between PFs and RFs, reporting new additional markers to distinguish between different fibroblast subtypes [1,20–24]. As a result of these new insights, our understanding of fibroblast heterogeneity is becoming increasingly complex. However, to this date information is scarce on the effect of TGF-β modulation on the different fibroblast subsets in HTSs or fibrosis in general. Moreover, it is unknown to what extent this affects the function of the different fibroblast subtypes. For this reason, we assessed the effects of exon skipping on morphology, gene and protein expression profiles of the different fibroblast cultures. In addition, we investigated the behaviour of the different fibroblast cultures with respect to contraction upon exon skipping. Especially PFs, residing in the superficial dermis, were of great interest, since it has been reported that superficial dermal fibroblasts are anti-fibrotic [12].

Exon skipping revealed a spindle shape- like appearance in the TGF-β1 stimulated groups in all fibroblast cultures, hence resembling PFs. This effect was less pronounced at basal levels. A possible explanation for this result could be addressed to the fact that dermal fibroblasts express persistent levels of ALK5 during wound healing and hypertrophic scars [25]. Furthermore, HTSs exhibit high concentrations of myofibroblast abundance [25,26]. Together, this could explain why fibroblasts start to express higher levels of ALK5 in a fibrotic environment, thus after TGF-β1 activation, and therefore being more susceptible for exon skipping of the ALK5 ligand binding domain. Gene expression analysis confirmed that the effect of ALK5 exon skipping on the markers of the pro-fibrotic RFs and MFs was most pronounced in the TGF-β1- stimulated samples. In addition, the fibrotic effect found after TGF-β1 was in agreement with a previous study that reported that TGF-β1-treated PFs differentiation towards RFs. This was confirmed by a significant downregulation of papillary markers NTN1 and PDPN together with an upregulation of reticular and myofibroblast markers CNN1, CDH2, TGM2 and αSMA [4]. One would expect that after exon skipping PF markers would show an upregulation of mRNA expression levels. Unexpectedly, this was only the case for PF marker CCRL1. NTN1, PDPN and TNC were not affected or even downregulated. Although the function of these markers in PFs still has to be elucidated fully, one could hypothesize that NTN1 and PDPN are downregulated by modulation of the TGF-β signalling pathway by e.g., ALK5 exon skipping. With regard to PF marker gene expression and the potentially anti-fibrotic, spindle shape-like appearance we found that in all cases of the anti-fibrotic phenotype CCRL1 was highly upregulated. This result could indicate that CCRL1 correlates with the re-appearance of PF-like fibroblasts after ALK5 inhibition, and potentially an anti-fibrotic phenotype. One way to confirm whether the PF-like cells indeed possess anti-fibrotic characteristics as described in literature, would be to determine decorin expression before and after re-activation with TGF-β1. Since decorin hampers TGF-β1 signalling, activation of TGF-β downstream targets should be reduced in these fibroblast cultures [44,45].

Next, we assessed protein expression of fibroblast markers TNC, TGM2 and αSMA. The rationale behind the selection of different markers was based on previous studies conducted by Janson and colleagues who used these markers successfully for western blot analysis to differentiate between PFs, RFs and MFs [4,27].

In contrast to earlier findings that showed distinct in vitro TNC expression levels between PFs (high) and RFs (low), it was striking to find that this marker showed considerable weak protein expression in our non-TGF-β stimulated PF cultures [1,2]. Speculatively TNC expression could change in PF cultures after prolonged culturing, thus reducing in activity over time. Moreover, when PFs were stimulated with TGF-β1, TNC expression was substantially elevated. A possible explanation for this apparently opposite effect could be derived from previous studies that have found a similar effect of TGF-β1 on TNC expression in human dermal fibroblasts by activation of the *Tnc* promotor through binding SMAD2 and SMAD3 [28,29]. Remarkably, we observed that PF marker TNC was downregulated after exon skipping in the TGF-β1-stimulated groups in all three fibroblast cultures. However, according to the observed changes in fibroblast morphology towards a PF-like phenotype, we expected TNC to be upregulated after exon skipping. Moreover, *de novo* TNC expression has been described to be a hallmark of inflammation, thus during the inflammatory phase of wound healing [30]. Furthermore, it has been reported that TNC expression is inhibited after normal scar development and shows persistence during HTS development [31]. Thus, although TNC is considered a marker of the papillary dermis and PFs, it has been suggested that TNC could also be a pro-fibrotic component, which could be downregulated using exon skipping as reported in our present study. RF marker TGM2 did not show any major changes at basal and TGF-β1 activated conditions. A previous study, conducted by Janson and colleagues, TGM2 expression was found to be higher in most RF monocultures compared to PF cultures at protein level [1]. Therefore, we selected TGM2 as a RF marker to assess its expression using western blot. However, in contrast with differential expression found in the study of Janson et al., we found no differences between PFs and RFs for TGM2. Further, in contrast with earlier findings and TGM2 gene expression in this study, no elevated TGM2 expression was found after TGF-β1 stimulation [4,32]. Based on protein data, it seems that TGM2 was not a suitable marker in this study, compared to previous studies. Therefore, it is warranted to use other RF markers for future experimentation, for example CNN1 [1]. Furthermore, ALK5 exon skipping reduced αSMA expression in the TGF-β- activated groups in the different fibroblast cultures. However, the scrambled AON sequence showed a similar reduction of αSMA. This observation suggests that the vivo-morpholino itself is primarily responsible for this effect on αSMA [33]. In order to observe a considerably effect of ALK5ViM, one could increase ViM concentrations and/or extend culturing. However, in the case of increasing AON concentration one should be careful, since ViMs could cause cytotoxicity at higher concentrations [33,34]. Strikingly, pharmacological ALK5 inhibition even showed upregulation

Please cite this article in press as: R.S. Raktoe, et al., The effect of TGFβRI inhibition on fibroblast heterogeneity in hypertrophic scar 2D *in vitro* models, Burns (2021), https://doi.org/10.1016/j.burns.2021.01.004

of αSMA in the TGF-β-stimulated groups of the RF and SF cultures. This effect could be explained by the difference in inhibition of the TGF-β signalling pathway by ALK5ViM and SB431542: ALK5ViM is able to inhibit the TGF-β-dependent SMAD and TGF-β- independent mitogen-activated protein kinase (MAPK) signalling pathway. Whereas SB431542 only inhibits the SMAD- dependent signalling pathway [35,36]. Therefore, upon SB431542 treatment in the TGF-β-activated group the inhibitory effect SMDAD2/3 inhibition is bypassed by a possible overactivation of MAPK in RF and SF cultures. This phenomenon could also explain the differential effect on gene expression between ALKViM and SB431542: CNN1, CDH2 and TGM2 are all associated with TGF-β signalling [37–40]. Since ALK5 exon skipping inhibits both canonical and non-canonical TGF-β signalling, we found more consistent downregulation of these pro-fibrotic RF markers. As mentioned earlier, PF markers also showed differential expression depending on exon skipping or pharmacological inhibition. Another explanation for this observation could be that activation of TGF-β signalling in an ALK5-independent manner [41,42]. Additional western blot analyses of basal expression levels of PDPN (PF), CDH2 (RF) and αSMA (MF) revealed that PF cultures primarily express PDPN, whereas RF and SF cultures both possess high expression levels of CDH2 and αSMA (Supplementary Figure S1), thus suggesting that PDPN and CHD2 should be taken along in further experimentation with a broader fibroblast biomarker panel. Altogether, these hypotheses require further investigation. Furthermore, a more elaborate fibroblast marker panel should be included in the experiments in order to elucidate the effect of ALK5 inhibition on the different fibroblast subtypes.

As confirmed by conducting a collagen gel contraction assay, we found that exon skipping was able to significantly reduce contraction and counteract TGF-β1-induced contraction, compared to control conditions. In agreement with the hypothesis that PFs exhibit anti-fibrotic features, we found that PF-embedded collagen gels showed overall significant lower contraction compared to collagen gels embedded with RFs and SFs at basal level and after TGF-β1 activation ($P < 0.001$) [43]. This finding could suggest that PFs are able to inhibit activated TGF-β1 residing in the ECM through the actions of decorin, which has been reported to be primarily expressed in the papillary dermis and is known to inhibit actions of TGF-β144,45]. In addition, reduced decorin expression is linked to HTS development [46].

Furthermore, contraction of FPCLs embedded with RFs resembled the contraction of SF-embedded lattices. This finding supports the resemblance of RFs and MFs, since the SF cultures also harbour MFs. In the study performed by Janson and colleagues, it has been proposed that RFs harbour low αSMA expression and, therefore, showing a more differentiated state compared to PFs. Thus, making RFs more prone to differentiating into MFs. In addition, several validated RF markers are associated with MFs [47–49]. In agreement with these findings, we observed higher αSMA expression in RF and SF containing FPCLs compared to PF-containing FPCLs. Further, αSMA expression followed contraction observed in the FPCLs and was reduced by ALK5 exon skipping especially in the TGF-β- stimulated groups. Moreover, human skin equivalents embedded with RFs showed higher contraction compared to those embedded with PFs [1]. Therefore, it would be of great interest to assess the effect of ALK5 exon skipping on different fibroblasts populations in a more advanced 3D model, such as human skin equivalents.

Considering the differentiation of PFs into MFs one can appreciate that this is a step-wise process in which the PFs differentiate into an intermediate state: the RF. However, proof that this process is probably more nuanced is the presence of so-called proto-MFs [50]. It has been proposed by Tomasek and colleagues that during wound healing fibroblasts differentiate to proto-MFs, primarily under mechanical tension caused by fibroblasts migrating via professional collagen bundles towards the wound bed. Next, TGF-β1 causes differentiation to mature MF [50]. The main difference between a proto-MF and mature MF is the former lacks αSMA expression and only expresses cytoplasmic β and γ actins. Therefore, by combining our findings together with data reported in the previous studies by Janson et al. and Tomasek et al., we propose that upon wound healing (and eventual HTS formation by MF persistence) PFs differentiate, due to tensional forces, into fibroblasts that express stress fibres that only express cytoplasmic β and γ actins (proto- MF) [1,50]. Next, TGF-β1 secreted by proto-MFs together with activated extracellular TGF-β1 and ongoing tensional forces ensure differentiation into RFs, expressing low levels of αSMA. Because of persistent mechanical stress and TGF-β1 secretion, the RFs differentiate into mature MFs [4,50–53]. Furthermore, a recent study reported the identification of functionally distinct fibroblast populations in the lower dermis and reticular dermis, of which two subtypes were reported to be as yet uncharacterized fibroblast subpopulations and could provide new insights on the presence and location of the proto-MFs, since it is known that the reticular dermis shows low MF abundance and thereby possibly presence of proto-MFs [23].

Altogether, our findings show that we were able to reduce presence of pro-fibrotic features in the heterogeneous SF population using exon skipping. In addition, we were able to maintain the desirable features to establish proper wound healing. In order to determine the stability of the phenotypes of the different fibroblast cultures, together with their specific features, it is warranted to continue with longevity studies. Phenotype studies could be conducted in 2D culture models. The long-term effects could be studied in 3D human skin equivalents, such as fibroblast-derived matrix models which could be established with PFs, RFs or SFs [54]. Furthermore, it would be of great interest to assess whether our approach could be useful in establishing skin substitutes in order to treat burn victims and, thereby, reducing severe scarring or even a step closer to scar-free wound healing.

Availability of data and material

All data generated and/or analyzed during this study are included in this published article.

Please cite this article in press as: R.S. Raktoe, et al., The effect of TGFβRI inhibition on fibroblast heterogeneity in hypertrophic scar 2D *in vitro* models, Burns (2021), https://doi.org/10.1016/j.burns.2021.01.004

Funding

This research was supported by the Dutch Burns Foundation (Grant number: NO. 14.105) located at Beverwijk, Netherlands.

Author's contributions

AEG, RVD and MKDJ were involved in the conception and design of the research. PPMVZ performed HS excisions and provided clinical knowledge. AEG, RVD and PPMVZ critically reviewed the manuscript. RS designed and carried out the experiments and analysis of the data for this study. MHR and JJOL participated in the experimental design and interpretation of the data. All authors read and approved the final manuscript.

Conflict of interest

None.

Appendix A. Supplementary data

Supplementary material related to this article can be found, in the online version, at doi:https://doi.org/10.1016/j.burns.2021.01.004.

REFERENCES

[1] Janson DG, Saintigny G, van Adrichem A, Mahé C, El Ghalbzouri A. Different gene expression patterns in human papillary and reticular fibroblasts. J Invest Dermatol [Internet] 2012;132(11)2565–72. . Available from: http://linkinghub.elsevier.com/retrieve/pii/S0022202X15355226.
[2] Darby I, Skalli O, Gabbiani G. Alpha-smooth muscle actin is transiently expressed by myofibroblasts during experimental wound healing. Lab Invest 1990;63(1):21–9.
[3] Hinz B. Formation and function of the myofibroblast during tissue repair. J Invest Dermatol 2007;127(3):526–37.
[4] Janson D, Saintigny G, Zeypveld J, Mahé C, El Ghalbzouri A. TGF-β1 induces differentiation of papillary fibroblasts to reticular fibroblasts in monolayer culture but not in human skin equivalents. Eur J Dermatol 2014;24(3):342–8.
[5] Desmoulière A, Redard M, Darby I, Gabbiani G. Apoptosis mediates the decrease in cellularity during the transition between granulation tissue and scar. Am J Pathol 1995;146(1):56–66.
[6] van der Veer WM, Bloemen MCT, Ulrich MMW, Molema G, van Zuijlen PP, Middelkoop E, et al. Potential cellular and molecular causes of hypertrophic scar formation. Burns 2009;35(1):15–29.
[7] Lee JY-Y, Yang C-C, Chao S-C, Wong T-W. Histopathological differential diagnosis of keloid and hypertrophic scar. Am J Dermatopathol 2004;26(5):379–84.
[8] Stunova A, Vistejnova L. Dermal fibroblasts—a heterogeneous population with regulatory function in wound healing. Cytokine Growth Factor Rev [Internet] 2018;39(January)137–50. . Available from: https://doi.org/10.1016/j.cytogfr.2018.01.003.
[9] Schafer I, Pandy M, Ferguson R, Davis B. Comparative observation of fibroblasts derived from the papillary and reticular dermis of infants and adults: growth kinetics, packing density at confluence and surface morphology. Mech Ageing Dev 1985;31:275–93.
[10] Sorrell JM, Baber MA, Caplan AI. Construction of a bilayered dermal equivalent containing human papillary and reticular dermal fibroblasts: use of fluorescent vital dyes. Tissue Eng 1996;2(1):39–49.
[11] Sorrell JM, Caplan AI. Fibroblast heterogeneity: more than skin deep. J Cell Sci 2004;117(Pt 5):667–75.
[12] Varkey M, Ding J, Tredget EE. Advances in skin substitutes-potential of tissue engineered skin for facilitating anti-fibrotic healing. J Funct Biomater 2015;6(3):547–63.
[13] Desmoulière A, Geinoz A, Gabbiani FGF. Transforming growth factor-beta 1 induces alpha-smooth muscle actin expression in granulation tissue myofibroblasts and in quiescent and growing cultured fibroblasts. J Cell Biol [Internet] 1993;122(1)103–11. . Available from: http://www.ncbi.nlm.nih.gov/pmc/articles/PMC2119614/.
[14] Ghahary A, Shen YJ, Scott PG, Tredget EE. Immunolocalization of TGF-beta 1 in human hypertrophic scar and normal dermal tissues. Cytokine 1995;7(2):184–90.
[15] Kemaladewi DU, Pasteuning S, van der Meulen JW, van Heiningen SH, van Ommen G-J, ten Dijke P, et al. Targeting TGF-β signaling by antisense oligonucleotide-mediated knockdown of TGF-β type I receptor. Mol Ther - Nucleic Acids [Internet] 2014;3(February)e156. . Available from: http://linkinghub.elsevier.com/retrieve/pii/S2162253116302992.
[16] Karkampouna S, Kruithof BP, Kloen P, Obdeijn MC, van der Laan AM, Tanke HJ, et al. Novel ex vivo culture method for the study of Dupuytren's disease: effects of TGFβ type 1 receptor modulation by antisense oligonucleotides. Mol Ther - Nucleic Acids [Internet] 2014;3(June 2013)e142. . Available from: http://linkinghub.elsevier.com/retrieve/pii/S2162253116302815.
[17] El Ghalbzouri A, Commandeur S, Rietveld MH, Mulder AA, Willemze R. Replacement of animal-derived collagen matrix by human fibroblast-derived dermal matrix for human skin equivalent products. Biomaterials [Internet] 2009;30(1)71–8. . Available from: https://doi.org/10.1016/j.biomaterials.2008.09.002.
[18] Smola H, Thiekotter G, Fusenig NE. Mutual induction of growth factor gene expression by epidermal-dermal cell interaction. J Cell Biol 1993;122(2):417–29.
[19] Janson D, Rietveld M, Mahé C, Saintigny G, El Ghalbzouri A. Differential effect of extracellular matrix derived from papillary and reticular fibroblasts on epidermal development in vitro. Eur J Dermatol 2017;27(3):237–46.
[20] Haydont V, Neiveyans V, Fortunel NO, Asselineau D. Transcriptome profiling of human papillary and reticular fibroblasts from adult interfollicular dermis pinpoints the 'tissue skeleton' gene network as a component of skin chrono-ageing. Mech Ageing Dev [Internet] 2019;179:60–77. . Available from: http://www.sciencedirect.com/science/article/pii/S0047637418301908.
[21] Haydont V, Neiveyans V, Perez P, Busson E, Lataillade J, Asselineau D, et al. Fibroblasts from the human skin dermo-hypodermal junction are distinct from dermal papillary and reticular fibroblasts and from mesenchymal stem cells and exhibit a specific molecular profile related to extracellular matrix organization and modeling. Cells 20209(2).
[22] Haydont V, Neiveyans V, Zucchi H, Fortunel NO, Asselineau D. Genome-wide profiling of adult human papillary and reticular fibroblasts identifies ACAN, Col XI α1, and PSG1 as general biomarkers of dermis ageing, and KANK4 as an exemplary effector of papillary fibroblast ageing, related to contractility. Mech Ageing Dev [Internet] 2019;177:157–81. . Available from: http://www.sciencedirect.com/science/article/pii/S0047637418300423.

[23] Philippeos C, Telerman SB, Oulès B, Pisco AO, Shaw TJ, Elgueta R, et al. Spatial and single-cell transcriptional profiling identifies functionally distinct human dermal fibroblast subpopulations. J Invest Dermatol 2018;138(4):811–25.
[24] Korosec A, Frech S, Gesslbauer B, Vierhapper M, Radtke C, Petzelbauer P, et al. Lineage identity and location within the dermis determine the function of papillary and reticular fibroblasts in human skin. J Invest Dermatol [Internet] 2019;139(2)342–51. . Available from: https://doi.org/10.1016/j.jid.2018.07.033.
[25] Schmid P, Itin P, Cherry G, Bi C, Cox DA. Enhanced expression of transforming growth factor-beta type I and type II receptors in wound granulation tissue and hypertrophic scar. Am J Pathol [Internet] 1998;152(2)485–93. . Available from: http://www.ncbiC.nlm.nih.gov/pubmed/9466575%5Cnhttp://www.pubmedcentral.nih.gov/articlerender.fcgi?artid=PMC1857945.
[26] Tuan T-L, Nichter LS. The molecular basis of keloid and hypertrophic scar formation. Mol Med Today 1998;4(1):19–24.
[27] Janson D, Rietveld M, Mahe C, Saintigny G, El Ghalbzouri A. Differential effect of extracellular matrix derived from papillary and reticular fibroblasts on epidermal development in vitro. Eur J Dermatol 2017;27(3):237–46.
[28] Pearson CA, Pearson D, Shibahara S, Hofsteenge J, Chiquet-ehrismann R. Tenascin: cDNA cloning and induction by TGF-beta. EMBO J 1988;7(10):2977–82.
[29] Jinnin M, Ihn H, Asano Y, Yamane K, Trojanowska M, Tamaki K. Tenascin-C upregulation by transforming growth factor-beta in human dermal fibroblasts involves Smad3, Sp1, and Ets1. Oncogene 200423:.
[30] Midwood KS, Chiquet M, Tucker RP, Orend G. Tenascin-C at a glance. J Cell Sci 2016129(23) 4321 LP – 4327.
[31] Dalkowski A, Schuppan D, Orfanos CE, Zouboulis CC. Increased expression of tenascin C by keloids in vivo and in vitro. Br J Dermatol. 1999;141(July (1)):50–6.
[32] Cao L, Shao M, Schilder J, Guise T, Mohammad KS, Matei D. Tissue transglutaminase links TGF-beta, epithelial to mesenchymal transition and a stem cell phenotype in ovarian cancer. Oncogene 2012;31(20):2521–34.
[33] Raktoe Rajiv S, Rietveld Marion H, Out-Luiting Jacoba J, Julio Marianna Kruithof-de, Zuijlen Paul PMvan, Remco van Doorn AEG. Exon skipping of TGFβRI affects signalling and ECM expression in hypertrophic scar-derived fibroblasts. Scars Burn Heal. 2020.
[34] Moulton JD. Guide for morpholino users: toward therapeutics. J Drug Discov Dev Deliv. 2016;3(2):1023.
[35] Sorrentino A, Thakur N, Grimsby S, Marcusson A, von Bulow V, Schuster N, et al. The type I TGF-β receptor engages TRAF6 to activate TAK1 in a receptor kinase-independent manner. Nat Cell Biol [Internet] 2008;10(10)1199–207. . Available from: https://doi.org/10.1038/ncb1780.
[36] Il Kim S, Kwak JH, Na H-J, Kim JK, Ding Y, Choi ME. Transforming growth Factor-β (TGF-β1) activates TAK1 via TAB1-mediated autophosphorylation, independent of TGF-β receptor kinase activity in mesangial cells. J Biol Chem [Internet] 2009;284(33)22285–96. . Available from: http://www.ncbi.nlm.nih.gov/pmc/articles/PMC2755952/.
[37] Hossain MM, Hwang D-Y, Huang Q-Q, Sasaki Y, Jin J-P. Developmentally regulated expression of calponin isoforms and the effect of h2-calponin on cell proliferation. Am J Physiol Cell Physiol 2003;284(1):C156–67.
[38] Yang H, Wang L, Zhao J, Chen Y, Lei Z, Liu X, et al. TGF-β-activated SMAD3/4 complex transcriptionally upregulates N-cadherin expression in non-small cell lung cancer. Lung Cancer. 2015;87(3):249–57.
[39] Szondy Z, Korponay-Szabó I, Király R, Sarang Z, Tsay GJ. Transglutaminase 2 in human diseases. BioMedicine [Internet] 2017;7(3)15. . Available from: https://pubmed.ncbi.nlm.nih.gov/28840829.
[40] Ritter SJ, Davies PJ. Identification of a transforming growth factor-beta1/bone morphogenetic protein 4 (TGF-beta1/BMP4) response element within the mouse tissue transglutaminase gene promoter. J Biol Chem 1998;273(21):12798–806.
[41] Zhang W, Jiang Y, Wang Q, Ma X, Xiao Z, Zuo W, et al. Single-molecule imaging reveals transforming growth factor-beta-induced type II receptor dimerization. Proc Natl Acad Sci USA [Internet] 2009;106(37)15679–83. . Available from: http://www.pnas.org/content/106/37/15679.
[42] You HJ, Bruinsma MW, How T, Ostrander JH, Blobe GC. The type III TGF-β receptor signals through both Smad3 and the p38 MAP kinase pathways to contribute to inhibition of cell proliferation. Carcinogenesis 2007;28(12):2491–500.
[43] Schafer IA, Shapiro A, Kovach M, Lang C, Fratianne RB. The interaction of human papillary and reticular fibroblasts and human keratinocytes in the contraction of three-dimensional floating collagen lattices. Exp Cell Res 1989;183(1):112–25.
[44] Schönherr E, Beavan LA, Hausser H, Kresse H, Culp LA. Differences in decorin expression by papillary and reticular fibroblasts in vivo and in vitro. Biochem J 1993;290(Pt 3):893–9.
[45] Zhang Z, Garron TM, Li X-J, Liu Y, Zhang X, et al. Recombinant human decorin inhibits TGF-β1-induced contraction of collagen lattice by hypertrophic scar fibroblasts. Burns 2009;35(4):527–37.
[46] Honardoust D, Varkey M, Marcoux Y, Shankowsky HA, Tredget EE. Reduced decorin, fibromodulin, and transforming growth Factor-β3 in deep dermis leads to hypertrophic scarring. J Burn Care Res [Internet] 2012;33(2)218–27. . Available from: http://content.wkhealth.com/linkback/openurl?sid=WKPTLP:landingpage&an=01253092-201203000-00007.
[47] Tomasek JJ, Vaughan MB, Kropp BP, Gabbiani G, Martin MD, Haaksma CJ, et al. Contraction of myofibroblasts in granulation tissue is dependent on Rho/Rho kinase/myosin light chain phosphatase activity. Wound Repair Regen 2006;14(3):313–20.
[48] Kulkarni AA, Thatcher TH, Olsen KC, Maggirwar SB, Phipps RP, Sime PJ. PPAR-gamma ligands repress TGFbeta-induced myofibroblast differentiation by targeting the PI3K/Akt pathway: implications for therapy of fibrosis. PLoS One 2011;6(1):e15909.
[49] Huang L, Haylor JL, Hau Z, Jones RA, Vickers ME, Wagner B, et al. Transglutaminase inhibition ameliorates experimental diabetic nephropathy. Kidney Int 2009;76(4):383–94.
[50] Tomasek JJ, Gabbiani G, Hinz B, Chaponnier C, Brown RA. Myofibroblasts and mechano-regulation of connective tissue remodelling. Nat Rev Mol Cell Biol [Internet] 2002;3(5)349–63. . Available from: http://www.nature.com/doifinder/10.1038/nrm809.
[51] Janson D, Rietveld M, Willemze R, El Ghalbzouri A. Effects of serially passaged fibroblasts on dermal and epidermal morphogenesis in human skin equivalents. Biogerontology 2013;14(2):131–40.
[52] Vaughan MB, Howard EW, Tomasek JJ. Transforming growth Factor-β1 promotes the morphological and functional differentiation of the myofibroblast. Exp Cell Res [Internet] 2000;257(1)180–9. . Available from: http://linkinghub.elsevier.com/retrieve/pii/S0014482700948699.
[53] Gabbiani G. The myofibroblast in wound healing and fibrocontractive diseases. J Pathol 2003;200(4):500–3.
[54] Ghetti M, Topouzi H, Theocharidis G, Papa V, Williams G, Bondioli E, et al. Subpopulations of dermal skin fibroblasts secrete distinct extracellular matrix: implications for using skin substitutes in the clinic. Br J Dermatol 2018;179(2):381–93.

Please cite this article in press as: R.S. Raktoe, et al., The effect of TGFβRI inhibition on fibroblast heterogeneity in hypertrophic scar 2D *in vitro* models, Burns (2021), https://doi.org/10.1016/j.burns.2021.01.004